



Swansea University
Prifysgol Abertawe



Cronfa - Swansea University Open Access Repository

This is an author produced version of a paper published in :
Composite Structures

Cronfa URL for this paper:

<http://cronfa.swan.ac.uk/Record/cronfa26526>

Paper:

Dey, S., Naskar, S., Mukhopadhyay, T., Gohs, U., Spickenheuer, A., Bittrich, L., Sriramula, S., Adhikari, S. & Heinrich, G. (2016). Uncertain natural frequency analysis of composite plates including effect of noise – A polynomial neural network approach. *Composite Structures*, 143, 130-142.

<http://dx.doi.org/10.1016/j.compstruct.2016.02.007>

This article is brought to you by Swansea University. Any person downloading material is agreeing to abide by the terms of the repository licence. Authors are personally responsible for adhering to publisher restrictions or conditions. When uploading content they are required to comply with their publisher agreement and the SHERPA RoMEO database to judge whether or not it is copyright safe to add this version of the paper to this repository.

<http://www.swansea.ac.uk/iss/researchsupport/cronfa-support/>

Accepted Manuscript

Uncertain natural frequency analysis of composite plates including effect of noise – A polynomial neural network approach

S. Dey, S. Naskar, T. Mukhopadhyay, U. Gohs, A. Spickenheuer, L. Bittrich, S. Sriramula, S. Adhikari, G. Heinrich

PII: S0263-8223(16)30027-7

DOI: <http://dx.doi.org/10.1016/j.compstruct.2016.02.007>

Reference: COST 7219

To appear in: *Composite Structures*



Please cite this article as: Dey, S., Naskar, S., Mukhopadhyay, T., Gohs, U., Spickenheuer, A., Bittrich, L., Sriramula, S., Adhikari, S., Heinrich, G., Uncertain natural frequency analysis of composite plates including effect of noise – A polynomial neural network approach, *Composite Structures* (2016), doi: <http://dx.doi.org/10.1016/j.compstruct.2016.02.007>

This is a PDF file of an unedited manuscript that has been accepted for publication. As a service to our customers we are providing this early version of the manuscript. The manuscript will undergo copyediting, typesetting, and review of the resulting proof before it is published in its final form. Please note that during the production process errors may be discovered which could affect the content, and all legal disclaimers that apply to the journal pertain.

Uncertain natural frequency analysis of composite plates including effect of noise – A polynomial neural network approach

S. Dey^{1,*}, S. Naskar², T. Mukhopadhyay^{3*}, U. Gohs¹, A. Spickenheuer¹, L. Bittrich¹,
S. Sriramula², S. Adhikari³, G. Heinrich^{1,4}

¹ Leibniz-Institut für Polymerforschung Dresden e.V. (IPF), Germany

² School of Engineering, University of Aberdeen, United Kingdom

³ College of Engineering, Swansea University, United Kingdom

⁴ Technische Universität Dresden, Germany

* Corresponding author's e-mail: infosudip@gmail.com

Abstract

This paper presents the quantification of uncertain natural frequency for laminated composite plates by using a novel surrogate model. A group method of data handling in conjunction to polynomial neural network (PNN) is employed as surrogate for numerical model and is trained by using Latin hypercube sampling. Subsequently the effect of noise on a PNN based uncertainty quantification algorithm is explored in this study. The convergence of the proposed algorithm for stochastic natural frequency analysis of composite plates is verified and validated with original finite element method (FEM). Both individual and combined variation of stochastic input parameters are considered to address the influence on the output of interest. The sample size and computational cost are reduced by employing the present approach compared to direct Monte Carlo simulation (MCS).

Keywords. uncertainty quantification; polynomial neural network; stochastic natural frequency; Latin hypercube; composite plate

1. Introduction

Laminated composite plates are extensively used in aerospace, civil, marine and many other engineering applications due to the benefit of light-weightness without compromising its strength and stiffness requirement. As modern weight-sensitive structures made of composite materials require more critical and complex design, the need for an accurate approach to assess the underlying uncertainties in the model, geometry, material properties, manufacturing process and operational environments has increased significantly. In the conventional deterministic analysis of structures, the variations in the system parameters are neglected and mean values of system parameters are used in the analysis with some factor of safety that may often lead to a conservative design. Due to the dependency on a large number of parameters in complex production and fabrication processes of laminated composite plate, the system properties can be random in nature resulting in uncertainty in the response of the laminated composite plate. Therefore, to well define the original problems and enable a better understanding and characterization of the actual behavior of the laminated composite structures, it is of prime importance that the inherent randomness in system parameters is incorporated in the analysis. To establish the reliability of such structures, application of computational power has favored the development of high-fidelity finite element models to deal with industrial problems. In spite of advances in capacity and speed of computer, the enormous computational cost of running complex, high fidelity scientific and engineering simulations makes it impractical to rely exclusively on simulation codes for the purpose of uncertainty quantification. Hence these high-fidelity models however own the drawback that they can be very time consuming so that only a few runs of the model can be affordable. Thus these models are practically unusable in computationally intensive methods such as traditional Monte Carlo simulation based approach, which needs thousands of finite element simulations. To overcome this lacuna generally surrogate based approach is utilized for uncertainty quantification of computationally intensive models.

Considerable researches based on deterministic analysis have been carried out on free vibration analysis of composite plates using classical laminated plate theory (CLPT) [1], first order shear deformation theory (FSDT) [2], higher order shear deformation theory (HSDT) [3] and three-dimensional (3-D) elasticity theory [4]. A considerable volume of literature is available on different analyses of laminated composites considering both deterministic [5-8] and stochastic [9-12] approaches. Based on higher-order theory, Naveentraj et al. [13] studied the linear static response of graphite-epoxy composite laminates with randomness in material properties by using combination of finite element analysis and Monte Carlo simulation (MCS). Further Salim et al. [14] examined the effect of randomness in material properties such as elastic modulus Poisson's ratios etc. on the response statistics of a composite plate subjected to static loading using CLPT in conjunction with first order perturbation techniques (FOPT). Onkar and Yadav [15] investigated the nonlinear response statistics of composite-laminated flat panels with random material properties subjected to transverse random loading based on CLPT in conjunction with FOPT. Giunta et al. [16] studied the free vibration of composite plates using refined theories accounting for uncertainties. The random vibration problem deals with big data of several stochastic input parameters wherein the dimension of stiffness matrix and number of iteration reduces the computational efficacy. The curse of dimensionality is a potential challenge related with the fact that the convergence of any estimator to the true value of a smooth function defined on a space of high dimension is very slow. This means that, a priori, an ample amount of observations are required to obtain a good estimated function of the parameter of interest. This problem can be solved by using suitable reduced order model (ROM). Many researchers used ROM in different applications such as high dimensional model representation (HDMR) [17-18], Kriging [19-20], artificial neural network [21-22], polynomial regression model [23-25]. Fuzzy uncertainty propagation in composites using Gram-Schmidt polynomial chaos expansion is reported recently [26]. Relatively little efforts have been made in the past by the

researchers and investigators on using polynomial neural network (PNN) model for the prediction of random system properties. Zjavka [27] employed the polynomial neural network model for forecasting the correct wind speed while Gómez-Ramírez et al. [28] investigated on forecasting time series with a new architecture for polynomial artificial neural network. Zhang et al. [29] studied the cross-validation based weights and structural analysis by Chebyshev-polynomial neural networks. Xin et al. [30, 31] investigated on monotonicity and convergence of asynchronous update gradient method and with penalty using ridge polynomial neural network while Roh et al. [32, 33] studied on fuzzy linear regression and radial basis function based on PNN. Recently, Huang et al. [34], Oh et al. [35] and Fazel Zarandi et al. [36] also studied the fuzzy polynomial neural networks with respective applications. Maric [37] introduced the self-organizing polynomial neural networks for solving the optimization problem while Dorn et al. [38] studied on group method of data handling (GMDH) - polynomial neural network-based method to predict approximate three-dimensional structures of polypeptides. To the best of the authors' knowledge, there is no literature covering the uncertainty quantification of natural frequencies in laminated composite structures using the polynomial neural network model. Moreover, the analysis of noise on such surrogate based uncertainty quantification algorithms is first attempted in this study.

In the present study, stochastic natural frequencies of laminated composite plates are analyzed in the presence of small random variation in the systems input variables. A polynomial neural network model is developed to reduce the computational time with adequate level of accuracy. The finite element formulation in conjunction with PNN model is thereby utilized to map the variation of responses of interest for randomness in layer-wise input parameters with different level of noise.

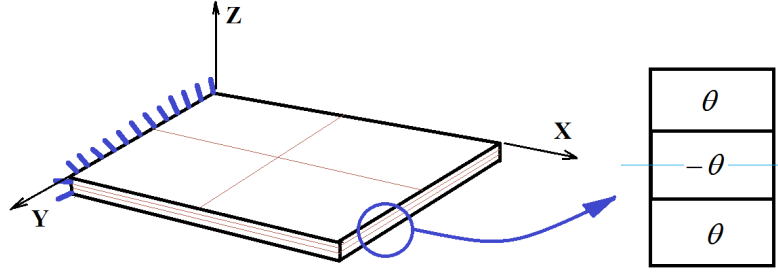


Fig. 1 Laminated composite cantilever plate

2. Mathematical formulation

Consider a rectangular composite laminated cantilever plate of uniform length L , width b , and thickness t , which consists of three plies located in a three-dimensional Cartesian coordinate system (x, y, z) , where the x - y plane passes through the middle of the plate thickness with its origin placed at the corner of the cantilever plate as shown in Figure 1. The composite plate is considered with uniform thickness with the principal material axes of each layer being arbitrarily oriented with respect to mid-plane. If the mid-plane forms the x - y plane of the reference plane, then the displacements can be computed as

$$\begin{aligned} u(x, y, z) &= u^0(x, y) - z\theta_x(x, y) \\ v(x, y, z) &= v^0(x, y) - z\theta_y(x, y) \\ w(x, y, z) &= w^0(x, y) = w(x, y), \end{aligned} \quad (1)$$

Assuming u , v and w are the displacement components in x -, y - and z -directions, respectively and u^0 , v^0 and w^0 are the mid-plane displacements, and θ_x and θ_y are rotations of cross-sections along the x - and y -axes. The strain-displacement relationships for small deformations can be expressed as

$$\begin{aligned} \epsilon_x &= \frac{\partial u^0}{\partial x} - z \frac{\partial^2 w^0}{\partial x^2}, & \epsilon_y &= \frac{\partial v^0}{\partial y} - z \frac{\partial^2 w^0}{\partial y^2} \\ \text{and } \gamma_{xy} &= \frac{\partial u^0}{\partial y} + \frac{\partial v^0}{\partial x} - z \frac{2 \partial^2 w^0}{\partial x \partial y} \end{aligned} \quad (2)$$

which in matrix form can be expressed as

$$\begin{Bmatrix} \varepsilon_x \\ \varepsilon_y \\ \gamma_{xy} \end{Bmatrix} = \begin{Bmatrix} \varepsilon_x^o \\ \varepsilon_y^o \\ \gamma_{xy}^o \end{Bmatrix} + z \begin{Bmatrix} k_x \\ k_y \\ k_{xy} \end{Bmatrix} \quad (3)$$

where $\varepsilon_x^o, \varepsilon_y^o, \gamma_{xy}^o$ are the strains in the reference plane and k_x, k_y, k_{xy} are the curvatures of reference plane of the plate. The random in-plane forces and moments acting on small element and the transverse shear forces (per unit length) are

$$\begin{aligned} N_x(\bar{\omega}) &= \int_{-t_b(\bar{\omega})}^{t_t(\bar{\omega})} \sigma_x dz, & N_y(\bar{\omega}) &= \int_{-t_b(\bar{\omega})}^{t_t(\bar{\omega})} \sigma_y dz, & N_{xy}(\bar{\omega}) &= \int_{-t_b(\bar{\omega})}^{t_t(\bar{\omega})} \tau_{xy} dz \\ M_x(\bar{\omega}) &= \int_{-t_b(\bar{\omega})}^{t_t(\bar{\omega})} z \sigma_x dz, & M_y(\bar{\omega}) &= \int_{-t_b(\bar{\omega})}^{t_t(\bar{\omega})} z \sigma_y dz, & M_{xy}(\bar{\omega}) &= \int_{-t_b(\bar{\omega})}^{t_t(\bar{\omega})} z \tau_{xy} dz \\ V_x(\bar{\omega}) &= \int_{-t_b}^{t_t} \tau_{xz} dz & \text{and} & & V_y(\bar{\omega}) &= \int_{-t_b}^{t_t} \tau_{yz} dz \end{aligned} \quad (4)$$

The stress-strain relationship for each ply can be expressed in matrix form

$$\begin{Bmatrix} \sigma_x \\ \sigma_y \\ \tau_{xy} \end{Bmatrix} = [\bar{Q}_{ij}(\bar{\omega})] \begin{Bmatrix} \varepsilon_x \\ \varepsilon_y \\ \gamma_{xy} \end{Bmatrix} \quad (5)$$

where $[\bar{Q}_{ij}(\bar{\omega})]$ is the stiffness matrix of the ply in x-y co-ordinate system and expressed as

$$[\bar{Q}_{ij}(\bar{\omega})] = \begin{bmatrix} m^4 & n^4 & 2m^2n^2 & 4m^2n^2 \\ n^4 & m^4 & 2m^2n^2 & 4m^2n^2 \\ m^2n^2 & m^2n^2 & (m^4 + n^4) & -4m^2n^2 \\ m^2n^2 & m^2n^2 & -2m^2n^2 & (m^2 - n^2) \\ m^3n & mn^3 & (mn^3 - m^3n) & 2(mn^3 - m^3n) \\ mn^3 & m^3n & (m^3n - mn^3) & 2(m^3n - mn^3) \end{bmatrix} [Q_{ij}] \quad (6)$$

Here $m = \sin \theta(\bar{\omega})$ and $n = \cos \theta(\bar{\omega})$, wherein $\theta(\bar{\omega})$ is the random fibre orientation angle.

However, laminate consists of a number of laminae wherein $[Q_{ij}]$ and $[\bar{Q}_{ij}(\bar{\omega})]$ denotes the on-axis elastic constant matrix and the off-axis elastic constant matrix, respectively. In matrix

form, the in-plane stress resultant $\{N\}$, the moment resultant $\{M\}$, and the transverse shear resultants $\{Q\}$ can be expressed as

$$\begin{aligned} \{N\} &= [A]\{\varepsilon^0\} + [B]\{k\} \quad \text{and} \quad \{M\} = [B]\{\varepsilon^0\} + [D]\{k\} \\ \{Q\} &= [A^*]\{\gamma\} \end{aligned} \quad (7)$$

$$[A_{ij}^*] = \int_{-t_b(\bar{\omega})}^{t_t(\bar{\omega})} \bar{Q}_{ij} dz \quad \text{where } i, j = 4, 5$$

The elasticity matrix of the laminated composite plate is given by,

$$[D'(\bar{\omega})] = \begin{bmatrix} A_{ij}(\bar{\omega}) & B_{ij}(\bar{\omega}) & 0 \\ B_{ij}(\bar{\omega}) & D_{ij}(\bar{\omega}) & 0 \\ 0 & 0 & S_{ij}(\bar{\omega}) \end{bmatrix} \quad (8)$$

where

$$[A_{ij}(\bar{\omega}), B_{ij}(\bar{\omega}), D_{ij}(\bar{\omega})] = \sum_{k=1}^n \int_{z_{k-1}}^{z_k} [\bar{Q}_{ij}(\bar{\omega})]_k [1, z, z^2] dz \quad i, j = 1, 2, 6 \quad (9)$$

$$[S_{ij}(\bar{\omega})] = \sum_{k=1}^n \int_{z_{k-1}}^{z_k} \alpha_s [\bar{Q}_{ij}(\bar{\omega})]_k dz \quad i, j = 4, 5 \quad (10)$$

where α_s is the shear correction factor and is assumed as 5/6. Now, the mass per unit area is denoted by P and is given by

$$P(\bar{\omega}) = \sum_{k=1}^n \int_{z_{k-1}}^{z_k} \rho(\bar{\omega}) dz \quad (11)$$

The element mass matrix is expressed as

$$[M_e(\bar{\omega})] = \int_{Vol} [N][P(\bar{\omega})][N] d(vol) \quad (12)$$

The element stiffness matrix is given by

$$[K_e(\bar{\omega})] = \int_{-1}^1 \int_{-1}^1 [B(\bar{\omega})]^T [D(\bar{\omega})] [B(\bar{\omega})] d\xi d\eta \quad (13)$$

The Hamilton's principle [39] is employed to study the dynamic nature of the composite structure. The principle used for the Lagrangian which is defined as

$L_f = T - U - W$ where T , U and W are total kinetic energy, total strain energy and total potential of the applied load, respectively. The Hamilton's principle applicable to non-conservative system can be expressed as,

$$\delta H = \int_{t_i}^{t_f} [\delta T - \delta U - \delta W] dt = 0 \quad (14)$$

The energy functional for Hamilton's principle is the Lagrangian (L_f) which includes kinetic energy (T) in addition to potential strain energy (U) of an elastic body. The expression for kinetic energy of an element is given by

$$T = \frac{1}{2} \{\dot{\delta}_e\}^T [M_e(\bar{\omega})] + [C_e(\bar{\omega})] \{\delta_e\} \quad (15)$$

The potential strain energy for an element of a plate can be expressed as,

$$U = U_1 + U_2 = \frac{1}{2} \{\delta_e\}^T [K_e(\bar{\omega})] \{\delta_e\} \quad (16)$$

The Lagrange's equation of motion is given by

$$\frac{d}{dt} \left[\frac{\partial L_f}{\partial \dot{\delta}_e} \right] - \left[\frac{\partial L_f}{\partial \delta_e} \right] = \{F_e\} \quad (17)$$

where $\{F_e\}$ is the applied external element force vector of an element and L_f is the Lagrangian function. Substituting $L_f = T - U$, and the corresponding expressions for T and U in Lagrange's equation, one obtains the dynamic equilibrium equation for free vibration of each element in the following form [40]

$$[M_e(\bar{\omega})] \{\ddot{\delta}_e\} + [K_e(\bar{\omega})] \{\delta_e\} = 0 \quad (18)$$

After assembling all the element matrices and the force vectors with respect to the common global coordinates, the resulting equilibrium equation is obtained. For the purpose of this study, the finite element model is developed for different element types and finite element discretization and nodal positions of the driving point and measurement point. Considering randomness of input parameters like ply-orientation angle, thickness, elastic modulus and

mass density etc., the equation of motion of a linear free vibration system with n degrees of freedom can be expressed as

$$[M(\bar{\omega})] \ddot{\delta}(t) + [K(\bar{\omega})] \delta(t) = 0 \quad (19)$$

where $K(\bar{\omega}) \in \mathbb{R}^{n \times n}$ is the elastic stiffness matrix, $M(\bar{\omega}) \in \mathbb{R}^{n \times n}$ is the mass matrix and $\delta(t) \in \mathbb{R}^n$ is the vector of generalized coordinates. The governing equations are derived based on Mindlin's theory incorporating rotary inertia, transverse shear deformation [41] using an eight-noded isoparametric plate bending element [42]. The composite cantilever plate is assumed to be under free vibration and the natural frequencies of the system are obtained as:

$$\omega_j^2(\bar{\omega}) = \frac{1}{\lambda_j(\bar{\omega})} \quad \text{where } j = 1, \dots, n_r \quad (20)$$

Here $\lambda_j(\bar{\omega})$ is the j -th eigenvalue of matrix $A = K^{-1}(\bar{\omega})M(\bar{\omega})$ and n_r indicates the number of modes retained in this analysis.

3. Polynomial neural network

In general, the Polynomial Neural Network (PNN) algorithm [43-45] is the advanced succession of Group Method of Data Handling (GMDH) method wherein different linear, modified quadratic, cubic polynomials are used. By choosing the most significant input variables and polynomial order among various types of forms available, the best partial description (PD) can be obtained based on selection of nodes of each layer and generation of additional layers until the best performance is reached. Such methodology leads to an optimal PNN structure wherein the input-output data set can be expressed as

$$(X_i, Y_i) = (x_{1i}, x_{2i}, x_{3i}, \dots, x_{ni}, y_i) \quad \text{where } i=1,2,3,\dots,n \quad (21)$$

By computing the polynomial regression equations for each pair of input variable x_i and x_j and output Y of the object system which desires to modeling

$$Y = A + Bx_i + Cx_j + Dx_i^2 + Ex_j^2 + Fx_ix_j \quad \text{where } i, j=1,2,3,\dots,n \quad (22)$$

where A, B, C, D, E, F are the coefficients of the polynomial equation. This provides $n(n-1)/2$ high-order variables for predicting the output Y in place of the original n variables (x_1, x_2, \dots, x_n) . After finding these regression equations from a set of input-output observations, we then find out which ones to save. This gives the best predicted collection of quadratic regression models. We now use each of the quadratic equations that we have just computed and generate new independent observations that will replace the original observations of the variables (x_1, x_2, \dots, x_n) . From these new independent variables we will combine them exactly as we did before. That is, we compute all of the quadratic regression equations of Y versus these new variables. This will provide a new collection of $n(n-1)/2$ regression equation for predicting Y from the new variables, which in turn are estimates of Y from above equations. Now the best of new estimates is selected to generate new independent variables from selected equations to replace the old, and combine all pair of these new variables. This process is continued until the regression equations begin to have a poorer predictability power than did the previous ones. In other words, it is the time when the model starts to become overfitted. The estimated output \hat{Y}_i can be further expressed as

$$\begin{aligned} \hat{Y} &= \hat{f}(x_1, x_2, x_3, \dots, x_n) \\ &= A_0 + \sum_{i=1}^n B_i x_i + \sum_{i=1}^n \sum_{j=1}^n C_{ij} x_i x_j + \sum_{i=1}^n \sum_{j=1}^n \sum_{k=1}^n D_{ijk} x_i x_j x_k + \dots \end{aligned} \quad (23)$$

where $i, j, k=1,2,3,\dots,n$

where $X(x_1, x_2, \dots, x_n)$ is the input variables vector and $P(A_0, B_i, C_{ij}, D_{ijk}, \dots)$ is vector of coefficients or weight of the Ivakhnenko polynomials. Components of the input vector X can be independent variables, functional forms or finite difference terms. This algorithm allows to find simultaneously the structure of model and model system output on the values of most

significant inputs of the system. The following steps are to be performed for the framework of the design procedure of PNN:

Step1: *Determination of input variables*: Define the input variables as $x_i = 1, 2, 3, \dots, n$ related to output variable Y . If required, the normalization of input data is also completed.

Step 2: *Create training and testing data*: Create the input–output data set (n) and divide into two parts, namely, training data (n_{train}) and testing data (n_{test}) where $n = n_{train} + n_{test}$. The training data set is employed to construct the PNN model including an estimation of the coefficients of the partial description of nodes situated in each layer of the PNN. Next, the testing data set is used to evaluate the estimated PNN model.

Step 3: *Selection of structure*: The structure of PNN is selected based on the number of input variables and the order of PD in each layer. Two kinds of PNN structures, namely a basic PNN and a modified PNN structure are distinguished. The basic taxonomy for the architectures of PNN structure is furnished in Figure 2.

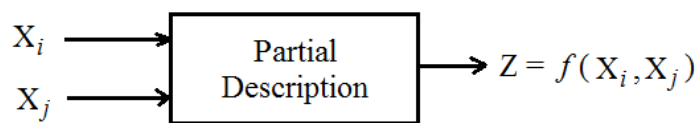


Fig. 2 Taxonomy for architectures of PNN

Step 4: *Determination of number of input variables and order of the polynomial*: Determine the regression polynomial structure of a PD related to PNN structure. The input variables of a node from n input variables $x_1, x_2, x_3, \dots, x_n$ are selected. The total number of PD s located at the current layer differs according to the number of the selected input variables from the nodes of the preceding layer. This results in $k = n! / (n - r)! r!$ nodes, where r is the

number of the chosen input variables. The choice of the input variables and the order of a *PD* itself help to select the best model with respect to the characteristics of the data, model design strategy, nonlinearity and predictive capability.

Step 5: *Estimation of coefficients of PD*: The vector of coefficients A_i is derived by minimizing the mean squared error between Y_i and \hat{Y}_i .

$$PI = \frac{1}{n_{train}} \sum_{i=1}^{n_{train}} (Y_i - \hat{Y}_i)^2 \quad (24)$$

where *PI* represents a criterion which uses the mean squared differences between the output data of original system and the output data of the model. Using the training data subset, this gives rise to the set of linear equations

$$Y = \sum_{i=1}^n X_i A_i \quad (25)$$

The coefficients of the *PD* of the processing nodes in each layer are derived in the form

$$A_i = [X_i^T X_i]^{-1} X_i^T Y \quad (26)$$

$$\text{where, } Y = [y_1, y_1, y_1, y_1, \dots, y_{n_{train}}]^T$$

$$X_i = [x_{1i}, x_{2i}, x_{3i}, \dots, x_{ki}, \dots, x_{train i}]^T$$

$$X_{ki}^T = [x_{ki1} \ x_{ki2} \dots \ x_{kin} \dots \ x_{ki1}^m \ x_{ki2}^m \dots \dots \ x_{kin}^m]^T$$

$$A_i = [A_{0i} \ A_{1i} \ A_{2i} \dots \dots \ A_{n'i}]^T$$

with the following notations i as the node number, k as the data number, n_{train} as the number of the training data subset, n as the number of the selected input variables, m as the maximum order, and n' as the number of estimated coefficients. This procedure is implemented repeatedly for all nodes of the layer and also for all layers of PNN starting from the input layer and moving to the output layer.

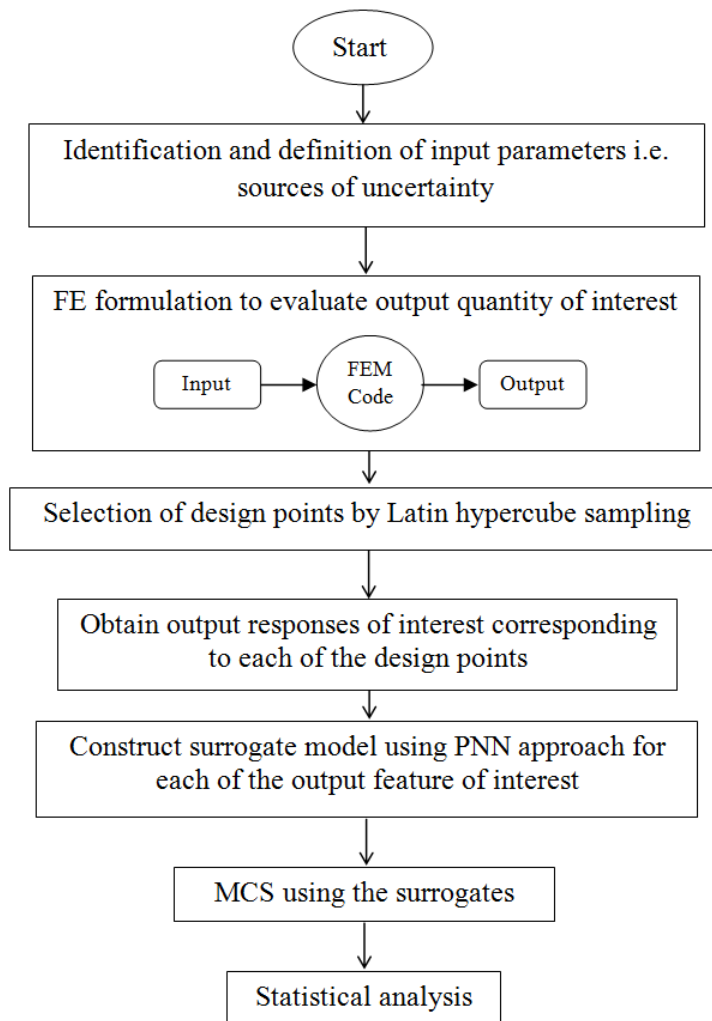


Fig. 3 Flowchart of stochastic natural frequency analysis using PNN model

Step 6: *Selection of PDs with the best predictive capability*: Each PD is estimated and evaluated using both the training and testing data sets. Then we compare these values and choose several PDs, which give the best predictive performance for the output variable.

Usually a predetermined number W of PDs is utilized.

Step 7: *Check the stopping criterion*: The stopping condition indicates that a sufficiently good PNN model is accomplished at the previous layer, and the modelling can be terminated. This

condition reads as $PI_j > PI^*$ where PI_j is a minimal identification error of the current layer whereas PI^* denotes a minimal identification error that occurred at the previous layer.

Step 8: *Determination of new input variables for the next layer*: If PI_j (the minimum value in the current layer) has not been satisfied (so the stopping criterion is not satisfied), the model has to be expanded. The outputs of the preserved *PDs* serve as new inputs to the next layer.

4. Stochastic approach using PNN model

Layer-wise stochasticity in material and geometric properties are considered as input parameters for stochastic natural frequency analysis of composite plates. The individual and combined cases of layer-wise random variations considered in the present analysis are as follows:

- (a) Variation of ply-orientation angle only: $\theta(\bar{\omega}) = \{\theta_1 \theta_2 \theta_3 \dots \theta_i \dots \theta_l\}$
- (b) Variation of thickness only: $t(\bar{\omega}) = \{t_1 t_2 t_3 \dots t_i \dots t_l\}$
- (c) Variation of elastic modulus only: $E_1(\bar{\omega}) = \{E_{1(1)} E_{1(2)} E_{1(3)} \dots E_{1(i)} \dots E_{1(l)}\}$
- (d) Variation of mass density only: $\rho(\bar{\omega}) = \{\rho_1 \rho_2 \rho_3 \dots \rho_i \dots \rho_l\}$
- (e) Combined variation of ply orientation angle, thickness, elastic modulus (longitudinal) and mass density:

$$g\{\theta(\bar{\omega}), t(\bar{\omega}), E_1(\bar{\omega}), \rho(\bar{\omega})\} = \{\Phi_1(\theta_1 \dots \theta_l), \Phi_2(t_1 \dots t_l), \Phi_3(E_{1(1)} \dots E_{1(l)}), \Phi_4(\rho_1 \dots \rho_l)\}$$

where θ_i , t_i , $E_{1(i)}$ and ρ_i are the ply orientation angle, thickness, elastic modulus along longitudinal direction and mass density, respectively and 'l' denotes the number of layer in the laminate. In the present study it is assumed that the distribution for randomness of input parameters exists within a certain band of tolerance with their deterministic values. $\pm 5^\circ$ for ply orientation angle and $\pm 10\%$ tolerance for material properties and thickness from deterministic values are considered. The flowchart of the proposed stochastic natural frequency analysis using PNN model is shown in Figure 3. Latin hypercube sampling [43] is

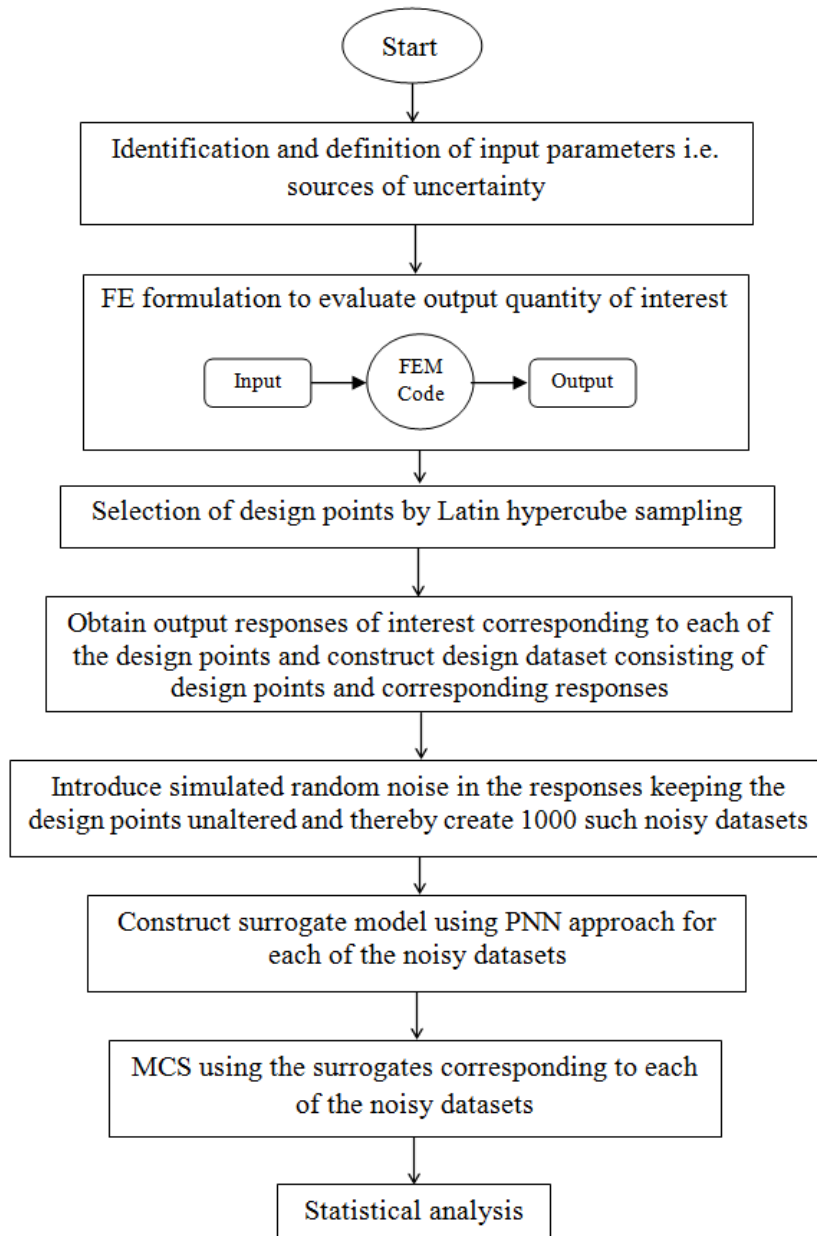


Fig. 4 Flowchart for analyzing the effect of noise on uncertainty quantification algorithm based on PNN

employed for generating sample points to ensure the representation of all portions of the vector space. In Latin hypercube sampling, the interval of each dimension is divided into m non-overlapping intervals having equal probability considering a uniform distribution, so the intervals should have equal size. Moreover, the sample is chosen randomly from a uniform distribution with a point in each interval, in each dimension and the random pair is selected

considering equal likely combinations for the point from each dimension. Subsequently to portray the effect of noise on the proposed PNN based uncertainty quantification algorithm, different levels of noise is introduced as described in Figure 4.

In the proposed approach, a Gaussian white noise with a specific multiplication factor (Var) is introduced in the set of output responses, which is used for PNN model formation

$$f_{ijN} = f_{ij} + \text{Var} \times \xi_{ij} \quad (28)$$

where f denotes natural frequency with the subscript i and j as frequency number and sample number, respectively. ξ_{ij} is a function that generates normally distributed random numbers. Subscript 'N' is used here to indicate the noisy frequency. Physical quantities that are expected to be the sum of many independent processes often have distributions that are nearly normal [46]. Therefore, Gaussian distribution has been adopted in this study to explore the effect of random noise. Thus, simulated noisy dataset (i.e. the sampling matrix for PNN model formation) is formed by introducing pseudo random noise in the responses, while the input design points are kept unaltered. Subsequently for each dataset, PNN based MCS is carried out to quantify the uncertainty of composite plates as described in Figure 4. Effects of noise are found to be accounted in several other studies in available literature [47-49] dealing with deterministic analysis. Recently noise is found to be accounted in uncertainty propagation using Kriging [50]. Assessment of PNN based uncertainty propagation algorithm under the effect of noise is the first attempt of its kind to the best of the authors' knowledge. The effect of such simulated noise can be regarded as considering other sources of uncertainty (except the commonly considered stochasticity in material and geometric parameters) such as error in measurement of responses, error in modelling and computer simulation and various other epistemic uncertainties involved with the system. It is difficult to quantitatively account the above mentioned sources of uncertainty and therefore, often ignored in most of the

available literature. Thus, the kind of analysis carried out here will provide a comprehensive idea about the robustness of PNN based uncertainty quantification algorithm under noisy data.

5. Results and Discussion

In this study, three layered graphite-epoxy symmetric angle-ply laminated composite cantilever plates are considered. The length, width and thickness of the composite laminate considered in the present analysis are 1 m, 1 m and 5 mm, respectively. Material properties of graphite-epoxy composite [51] considered with deterministic mean value as $E_1 = 138.0$ GPa, $E_2 = 8.96$ GPa, $G_{12} = 7.1$ GPa, $G_{13} = 7.1$ GPa, $G_{23} = 2.84$ GPa, $\mu = 0.3$, $\rho = 1600$ kg/m³. A discretization of (6 × 6) mesh on plan area with 36 elements 133 nodes with natural coordinates of an isoparametric quadratic plate bending element are considered for the present FEM approach. The finite element mesh size is finalized using a convergence study as shown in Table 1. For full scale MCS, the number of original finite element analysis is same as the sampling size. In general for complex composite structures, the performance function is not available as an explicit function of the random variables. The random response in terms of natural frequencies of the composite structure can only be evaluated numerically at the end of a structural analysis procedure such as the finite element method which is often time-consuming and computationally expensive. The present PNN method is employed to develop a predictive and representative surrogate model relating each natural frequency to a number of input variables. Thus the PNN model represents the result of structural analysis encompassing every possible combination of all stochastic input variables. From this mathematical model, thousands of combinations of all design variables can be created and performed using a pseudo analysis for each variable set, by adopting the corresponding predictive values.

Table 1 Convergence study for non-dimensional fundamental natural frequencies [$\omega = \omega_n L^2 \sqrt{(\rho/E_1 t^2)}$] of three layered ($\theta^\circ/-\theta^\circ/\theta^\circ$) graphite-epoxy composite plates, $a/b=1$, $b/t=100$, considering $E_1 = 138$ GPa, $E_2 = 8.96$ GPa, $G_{12} = 7.1$ GPa, $\mu = 0.3$.

| Ply angle, θ | Present FEM (4 × 4) | Present FEM (6 × 6) | Present FEM (8 × 8) | Present FEM (10 × 10) | Qatu and Leissa [52] |
|------------------------|------------------------|------------------------|------------------------|--------------------------|-------------------------|
| 0° | 1.0112 | 1.0133 | 1.0107 | 1.004 | 1.0175 |
| 45° | 0.4591 | 0.4603 | 0.4603 | 0.4604 | 0.4613 |
| 90° | 0.2553 | 0.2567 | 0.2547 | 0.2542 | 0.2590 |

A convergence study of sample size for PNN model formation with respect to direct MCS is shown in Table 2 for the first three stochastic natural frequencies due to individual and combined variation of ply-orientation angle, thickness, elastic modulus and mass density. It is a common practice to choose the sample size as 2^N , where N is a positive integer. In the present article we have shown typical results of convergence study for $N = 8, 9$ and 10 due to paucity of space. By analysing the statistical parameters presented in the Table 2 it is evident that sample size of 256 and 512 are adequate to form PNN model for individual and combined variation cases respectively.

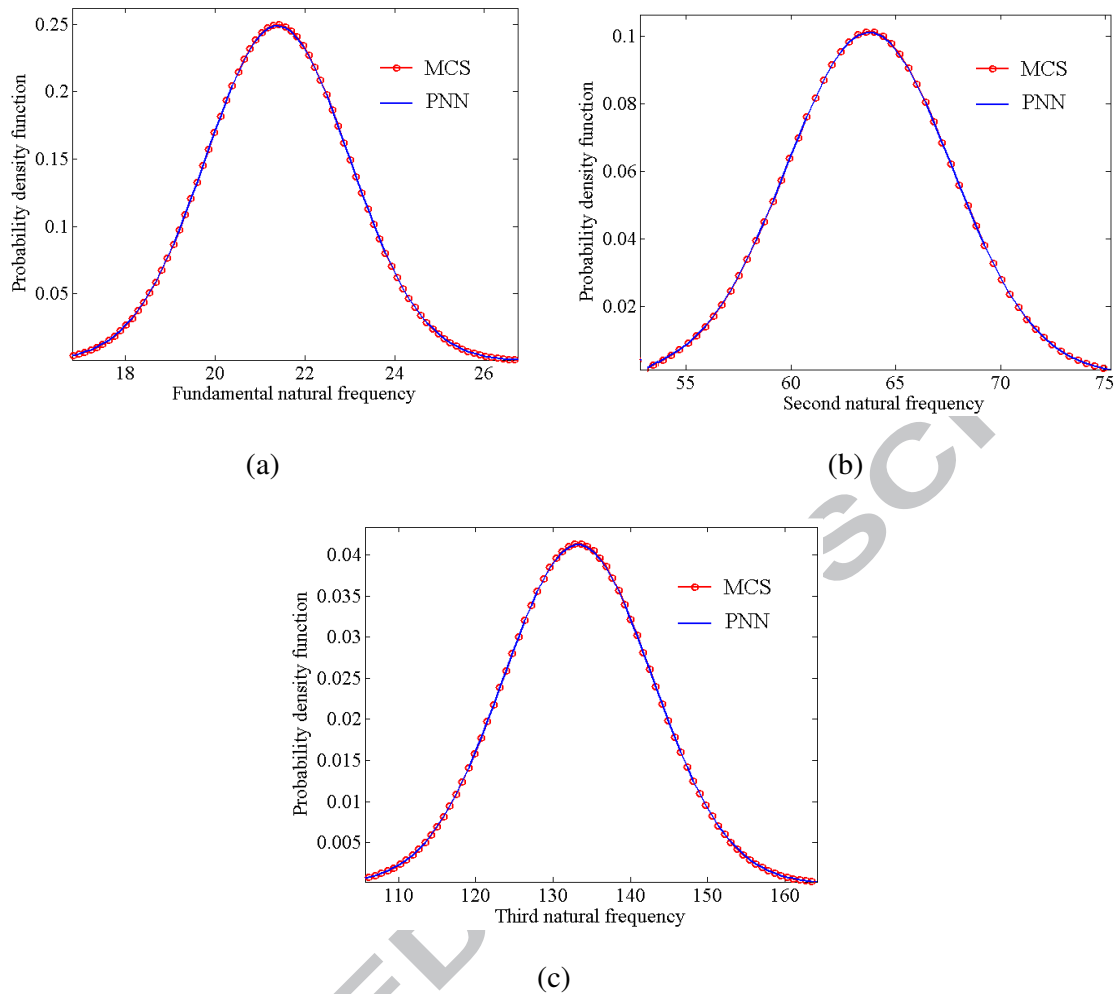


Fig. 5 Probability density function of first three stochastic natural frequencies (rad/s) using PNN approach for combined variation of ply angle, ply-thickness, longitudinal elastic modulus and mass density of angle-ply ($45^\circ/45^\circ/45^\circ$) composite cantilever plate

The probability density function (PDF) is plotted as the benchmark of bottom line results in this article. To illustrate the validation of results of the proposed PNN based approach with respect to direct MCS, natural frequencies corresponding to first three modes are considered. The probability density function plots comparing MCS with PNN and the scatter plots verifying the present PNN model corresponding to the first three modes are presented in Figure 5 and Figure 6 respectively. It is evident that the results of the proposed PNN based approach are in good agreement with that of direct MCS simulations corroborating accuracy of the proposed approach. Several new results for stochastic analysis

of composite plates are generated using the PNN based approach as presented in the subsequent paragraphs.

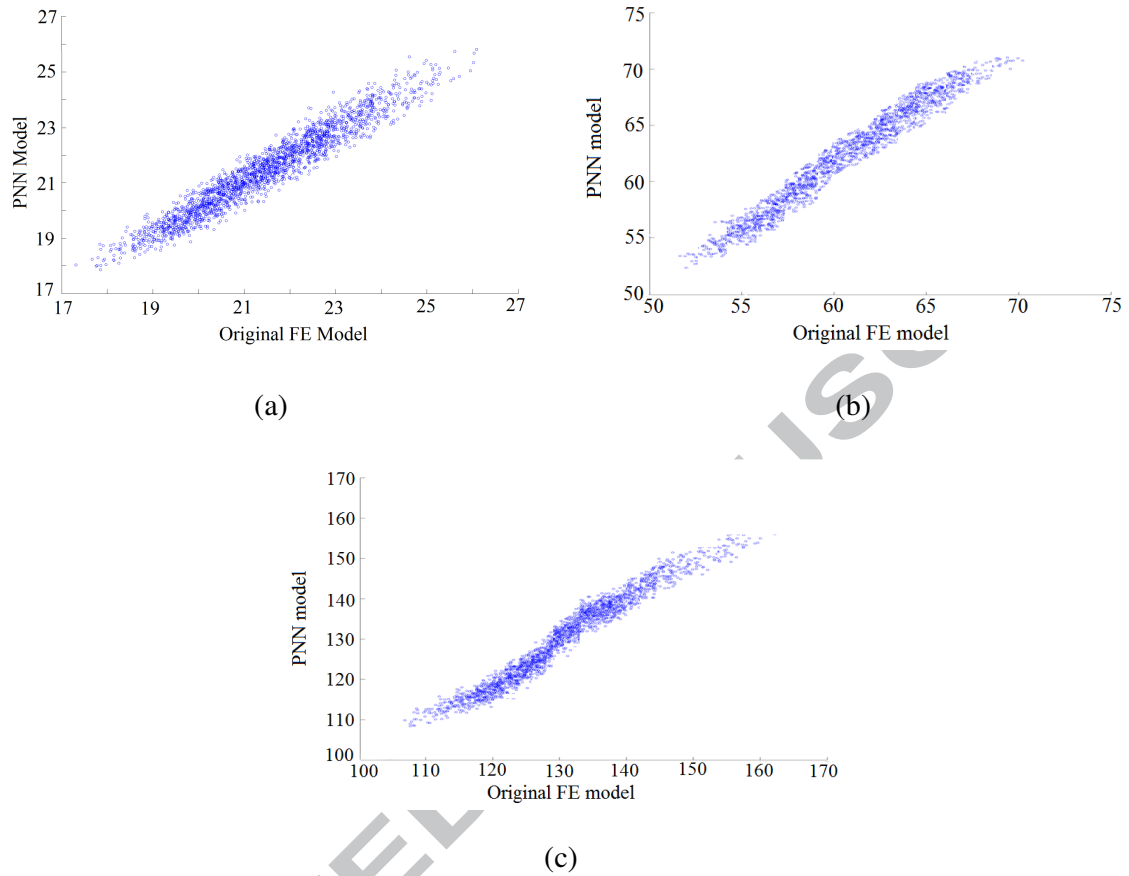


Fig. 6 Scatter plot for first three natural frequencies (rad/s) with respect to PNN model and original finite element model for combined variation of ply angle, ply-thickness, longitudinal elastic modulus and mass density of angle-ply ($45^\circ/-45^\circ/45^\circ$) composite cantilever plate.

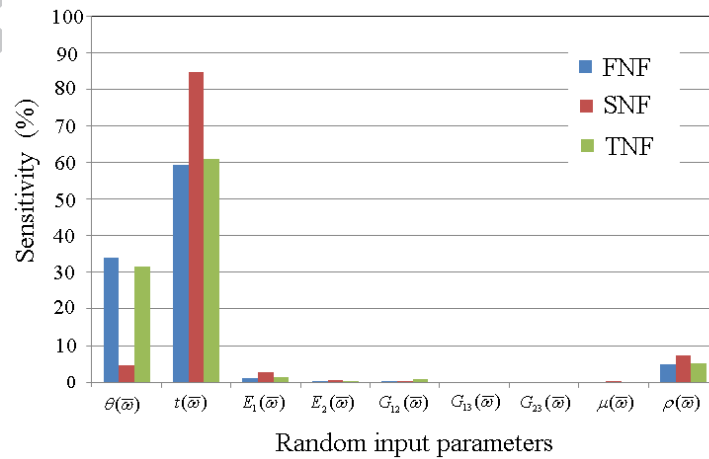


Fig. 7 Sensitivity of input parameters corresponding to fundamental (FNF), second (SNF) and third (TNF) natural frequencies for angle-ply ($45^\circ/-45^\circ/45^\circ$) composite cantilever plate.

As presented in figure 7, the four most sensitive input parameters are identified as ply orientation angle, longitudinal elastic modulus, thickness and mass density using variance based global sensitivity analysis [47] while, the variation of other input parameters such as transverse elastic modulus, shear moduli and Poisson's ratio are found to have very little or negligible contribution on stochasticity of first three natural frequencies. For this reason the above mentioned four most sensitive input parameters are considered for analyzing combined stochasticity in the present analysis. The probability density function with respect to first three stochastic natural frequencies are plotted in Figure 8 due to individual and combined variation of ply-orientation angle, thickness, elastic modulus and mass density for angle-ply composite cantilever plate. The combined variation of input parameters is observed to have the maximum influence on stochasticity of natural frequencies compared to individual variation of input parameters irrespective of modes. Moreover, this collective plots give a clear idea about the volatility in natural frequencies due to stochasticity in different individual parameters that in turn provides a sense of their relative influences on the responses of interest. The effect of degree of orthogonality on stochastic first three natural frequencies corresponding to combined variation of angle-ply ($45^\circ/-45^\circ/45^\circ$) composite cantilever plate is shown in Figure 9. It is observed that as the ratio of longitudinal elastic modulus to transverse

Table 2 Convergence study of first three natural frequencies (rad/s) due to individual and combined variation of ρ , E_1 , t_s and θ of elastic modulus and mass density for angle-ply ($45^\circ/-45^\circ/45^\circ$) composite cantilever plate

| Input variation | Values | f_1 | | | | f_2 | | | | MCS (10,000) |
|--|--------|-----------------|------------------|---------|---------|-----------------|------------------|---------|---------|-----------------|
| | | MCS (10,000) | PNN (Sample run) | | | MCS (10,000) | PNN (Sample run) | | | |
| | | | 256 | 512 | 1024 | | 256 | 512 | 1024 | |
| $\theta(\bar{\omega})$ | Max | 23.7997 | 23.5643 | 23.6540 | 24.0071 | 65.6675 | 65.5571 | 65.5471 | 65.6788 | 146.53 |
| | Min | 19.3219 | 19.4239 | 19.3018 | 19.3018 | 61.5809 | 61.8885 | 61.6920 | 61.6920 | 120.02 |
| | Mean | 21.4006 | 21.3656 | 21.4225 | 21.4033 | 63.7467 | 63.7190 | 63.7624 | 63.7468 | 133.29 |
| | SD | 0.9154 | 0.9342 | 0.9553 | 0.9412 | 0.8435 | 0.8522 | 0.8750 | 0.8567 | 5.397 |
| $t_s(\bar{\omega})$ | Max | 23.5059 | 23.4940 | 23.5030 | 23.5057 | 70.2353 | 70.2008 | 70.2268 | 70.2347 | 146.43 |
| | Min | 19.2412 | 19.2529 | 19.2416 | 19.2445 | 57.6165 | 57.6511 | 57.6179 | 57.6263 | 120.19 |
| | Mean | 21.3736 | 21.3740 | 21.3762 | 21.3710 | 63.9269 | 63.9280 | 63.9347 | 63.9192 | 133.31 |
| | SD | 1.2313 | 1.2332 | 1.2325 | 1.2334 | 3.6434 | 3.6489 | 3.6468 | 3.6495 | 7.577 |
| $E_1(\bar{\omega})$ | Max | 21.7663 | 21.8053 | 21.7723 | 21.8053 | 65.5082 | 65.6505 | 65.5334 | 65.6505 | 135.37 |
| | Min | 20.9694 | 20.9761 | 20.9342 | 20.9252 | 62.2682 | 62.3001 | 62.1369 | 62.1085 | 131.18 |
| | Mean | 21.3660 | 21.3623 | 21.3725 | 21.3666 | 63.8962 | 63.8856 | 63.9198 | 63.9002 | 133.27 |
| | SD | 0.1503 | 0.1617 | 0.1637 | 0.1645 | 0.5986 | 0.6491 | 0.6535 | 0.6501 | 0.833 |
| $\rho(\bar{\omega})$ | Max | 22.3574 | 22.3099 | 22.4109 | 22.4276 | 66.8698 | 66.7277 | 67.0298 | 67.0797 | 139.45 |
| | Min | 20.5627 | 20.4647 | 20.5257 | 20.4647 | 61.5019 | 61.2089 | 61.3913 | 61.2089 | 128.25 |
| | Mean | 21.3835 | 21.3857 | 21.3691 | 21.3820 | 63.9570 | 63.9636 | 63.9138 | 63.9524 | 133.37 |
| | SD | 0.3609 | 0.3614 | 0.3601 | 0.3579 | 0.9897 | 1.0810 | 1.0770 | 1.0707 | 2.063 |
| $\theta, t_s, E_1, \rho(\bar{\omega})$ | Max | 26.3531 | 25.8323 | 26.0243 | 26.0914 | 74.7603 | 72.5097 | 73.4380 | 74.2836 | 162.07 |
| | Min | 16.9109 | 18.0873 | 17.3134 | 17.3031 | 53.9388 | 54.7321 | 54.9025 | 54.9022 | 106.22 |
| | Mean | 21.3907 | 21.4701 | 21.4453 | 21.4557 | 63.7304 | 63.9235 | 63.9352 | 63.9335 | 133.24 |
| | SD | 1.6029 | 1.6241 | 1.5990 | 1.5759 | 3.9481 | 4.0223 | 4.0245 | 3.9509 | 9.678 |

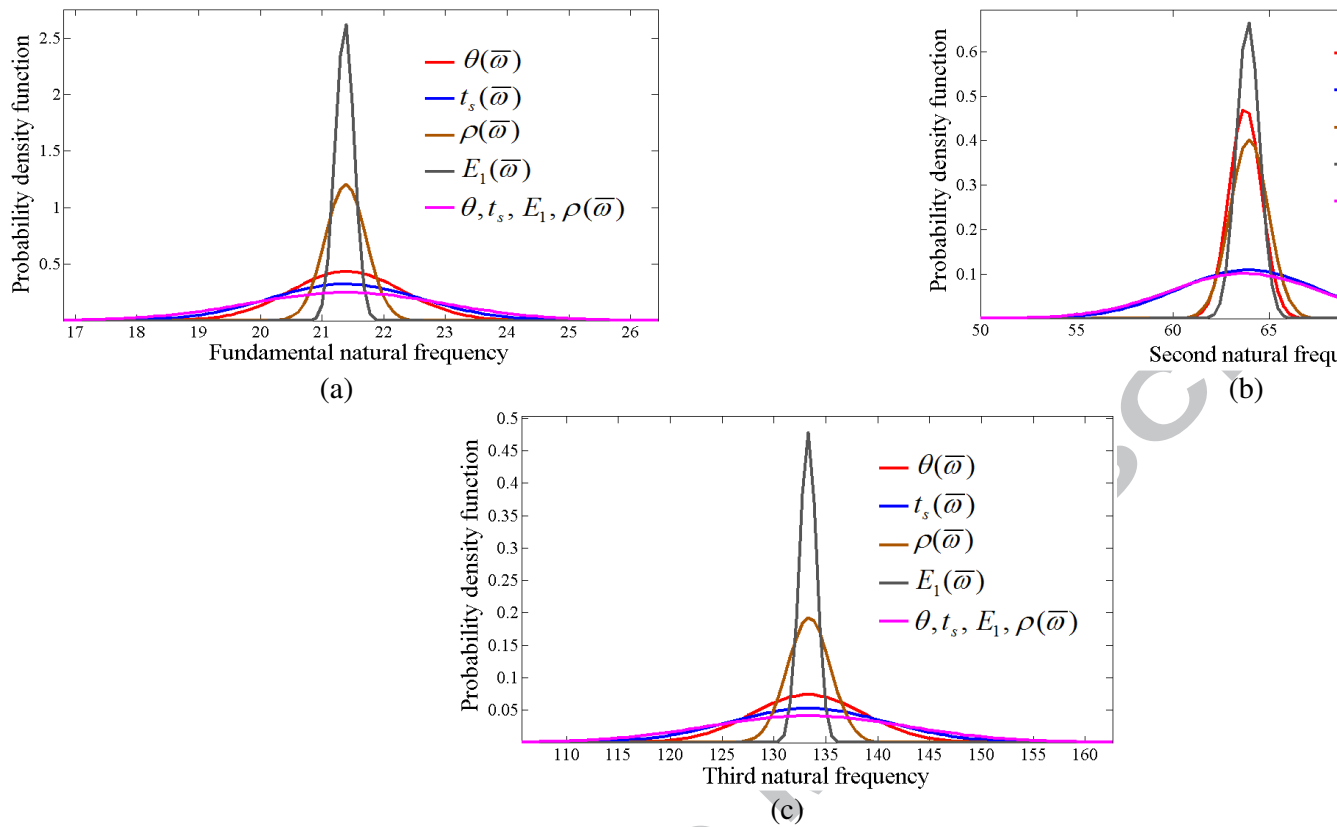


Fig. 8 Probability density function for first three natural frequencies (rad/s) due to individual and combined variations in thickness, elastic modulus and mass density for angle-ply ($45^\circ/-45^\circ/45^\circ$) composite cantilever plate.

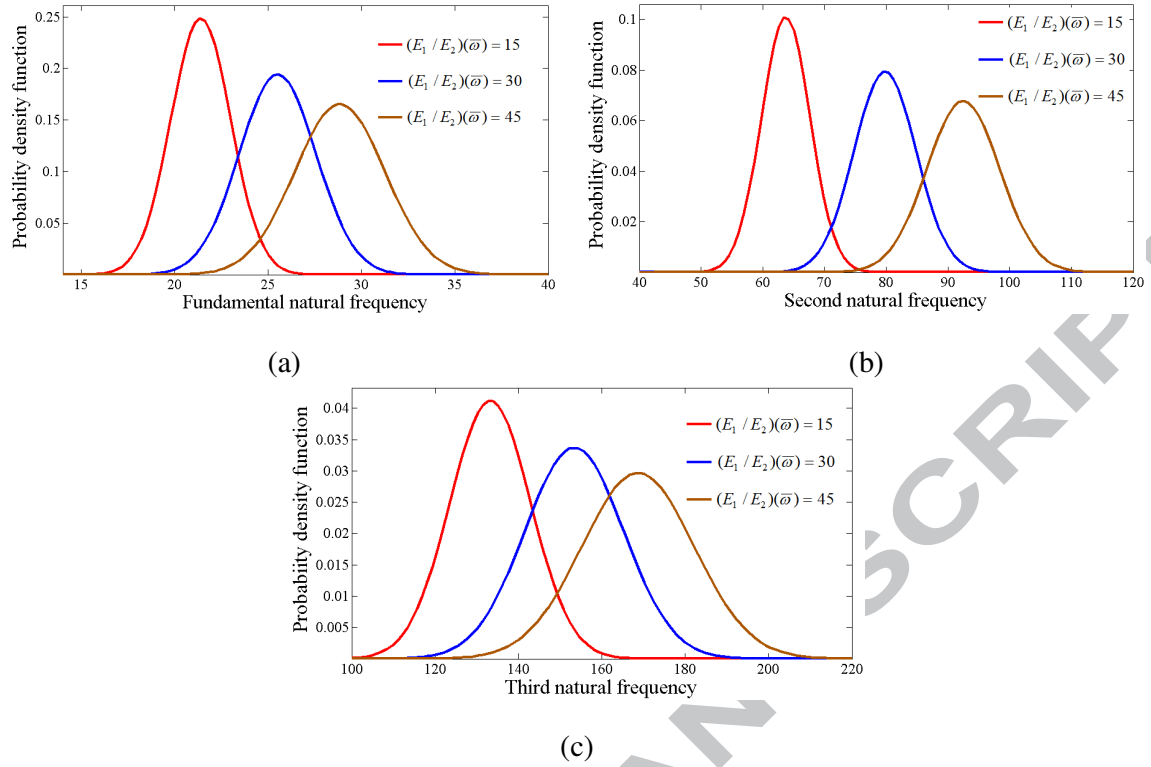


Fig. 9 Effect of degree of orthogonality on stochastic (a) fundamental (b) second and (c) third natural frequencies (rad/s) with respect to PNN model for combined variation of angle-ply ($45^\circ/-45^\circ/45^\circ$) composite cantilever plate.

elastic modulus increases the fluctuation of stochastic natural frequencies also proportionately increases irrespective of modes. To ascertain the degree of proportional variation, a comparative study is carried out to map the variation of stochastic natural frequencies due to variation in input parameters in case of combined variation case. Three cases are considered namely, (a) $\pm 5^\circ$ for ply orientation angle with subsequent $\pm 10\%$ tolerance for material properties (b) $\pm 10^\circ$ for ply orientation angle with subsequent $\pm 20\%$ tolerance for material properties and (c) $\pm 15^\circ$ for ply orientation angle with subsequent $\pm 20\%$ tolerance for material properties from respective deterministic mean values as depicted in Figure 10. It is evident that as the fluctuation of input parameters increases the sparsity of the stochastic output natural frequencies also increases while no notable variation of stochastic mean value of respective natural frequencies is identified due to the same.

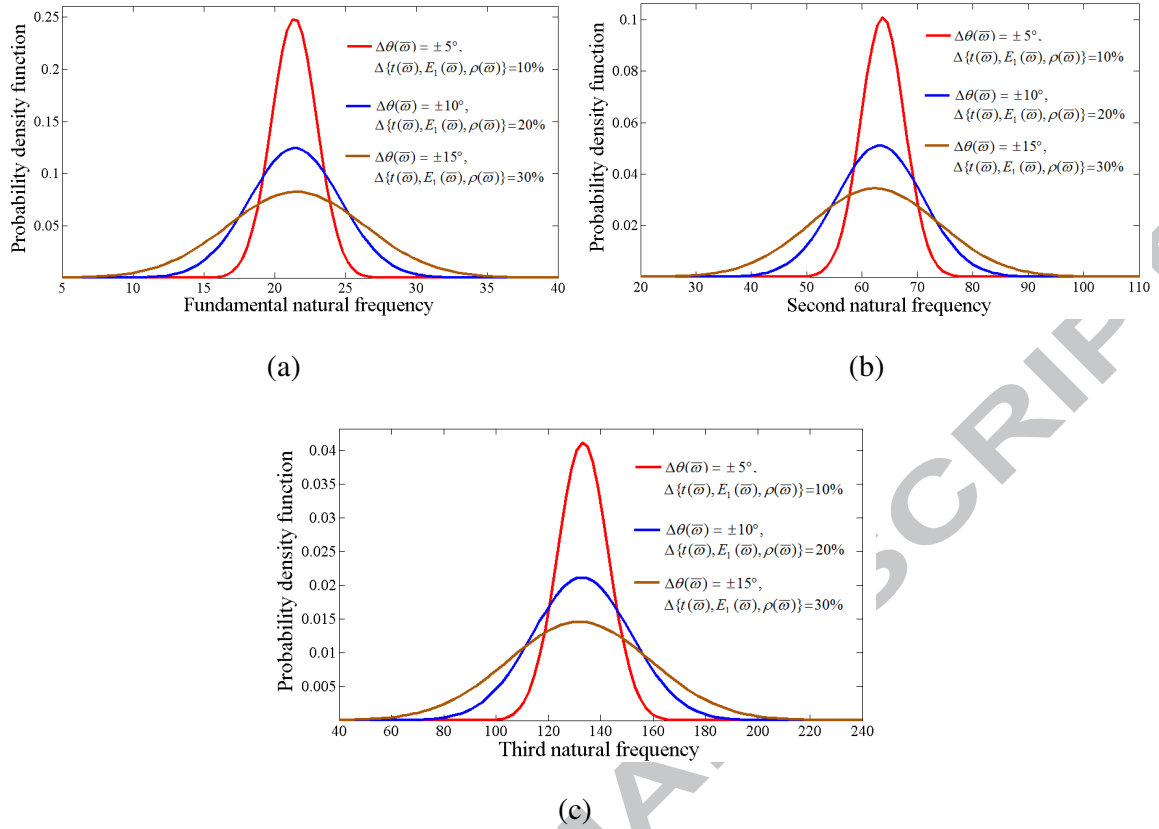


Fig. 10 Effect of variation of input parameters on stochastic (a) fundamental (b) second and (c) third natural frequencies (rad/s) with respect to PNN model for combined variation of angle-ply ($45^\circ/-45^\circ/45^\circ$) composite cantilever plate.

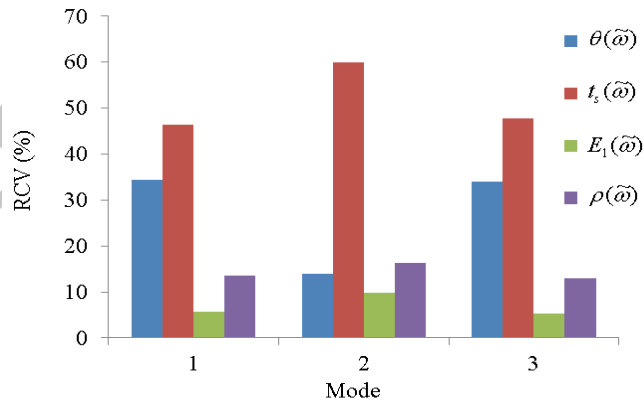


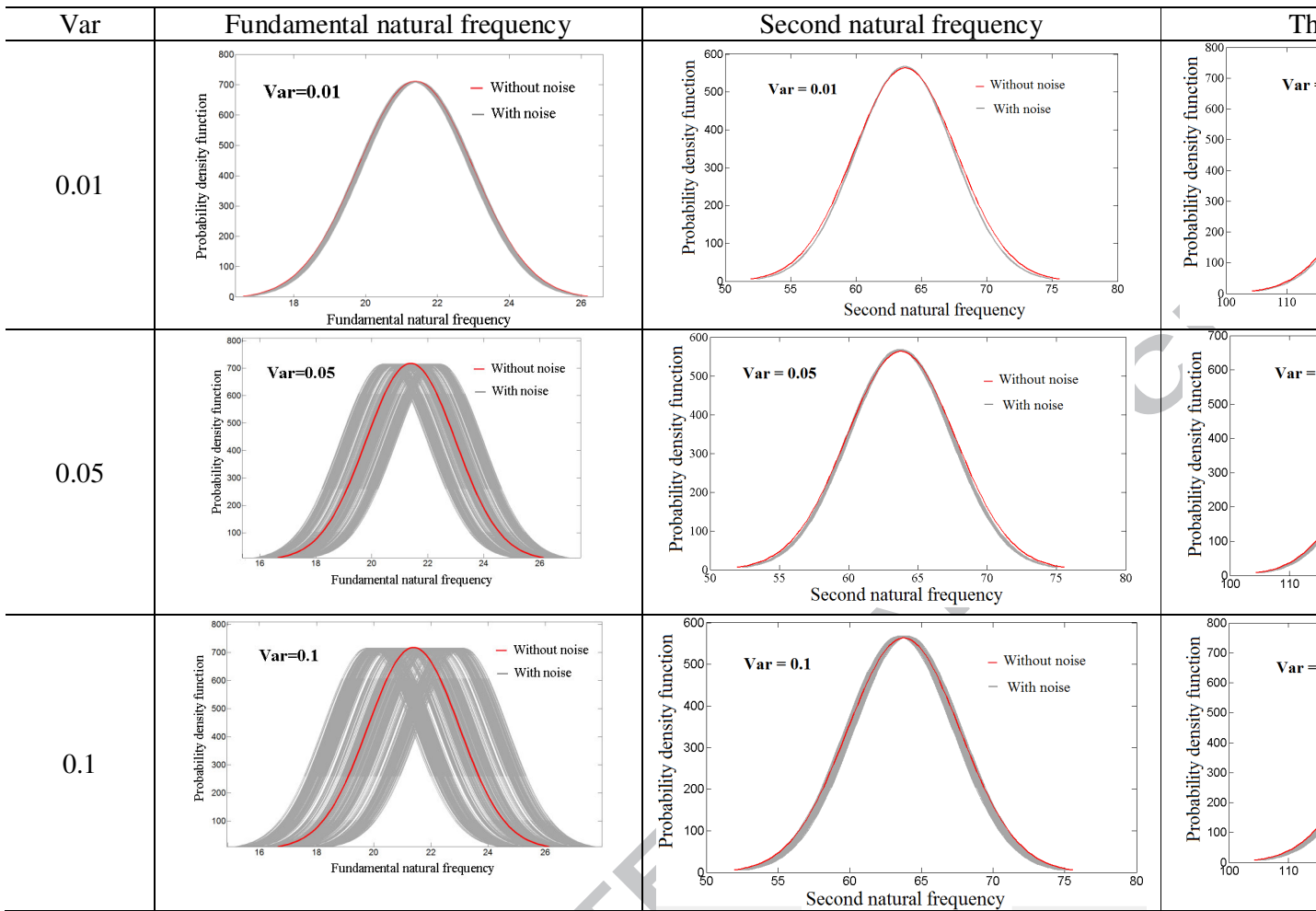
Fig. 11 Relative coefficient of variation (RCV) with respect to first three natural frequencies for angle-ply ($45^\circ/-45^\circ/45^\circ$) composite cantilever plate.

To map the contribution of individual input parameters due to their individual variation, the relative coefficient of variation (RCV) for first three modes of frequencies are

evaluated as shown in Figure 11. The thickness of each layer of the laminate is identified as the relatively most effective input parameter, followed by ply orientation angle, mass density and elastic modulus E_1 . It can be noted here that the results of RCV are in good agreement with figure 7. The effect of noise on PNN based uncertainty quantification algorithm (refer to Figure 4) for the case of combined variation of all stochastic input parameters is furnished in Figure 12. As the multiplication factor Var increases, the range of variations in the probability density function is also found to be increased. The fundamental natural frequency is identified to be the maximum noise-sensitive followed by the subsequent second and third natural frequencies. This is because of the fact that the range of magnitude increases with the increase in mode number and as magnitude of a particular frequency becomes higher the influence of same noise level would be lesser on that frequency.

6. Conclusions

The novelty of the present study includes incorporation of polynomial neural network based uncertainty propagation algorithm in laminated composite plates. Stochastic natural frequencies are analyzed considering layer-wise variation of individual as well as combined cases for random input parameters. Subsequently, the effect of noise on the proposed approach of uncertainty quantification is addressed. In this study, the uncertainty quantification of natural frequencies with uniform random input variables (such as ply orientation, ply-thickness and material properties) is formulated implicitly using finite element method and thereby PNN approach is incorporated to achieve computational efficiency. The computational time and cost is reduced by using the present PNN approach compared to conventional Monte Carlo simulation method. From the analyses presented in this article it is found that, as the percentage of variation of input parameters increases, the sparsity of the stochastic output natural frequencies also increases while no notable variation of stochastic mean value of respective natural frequencies is identified. The thickness parameter is found to be the most sensitive input parameter while longitudinal elastic modulus



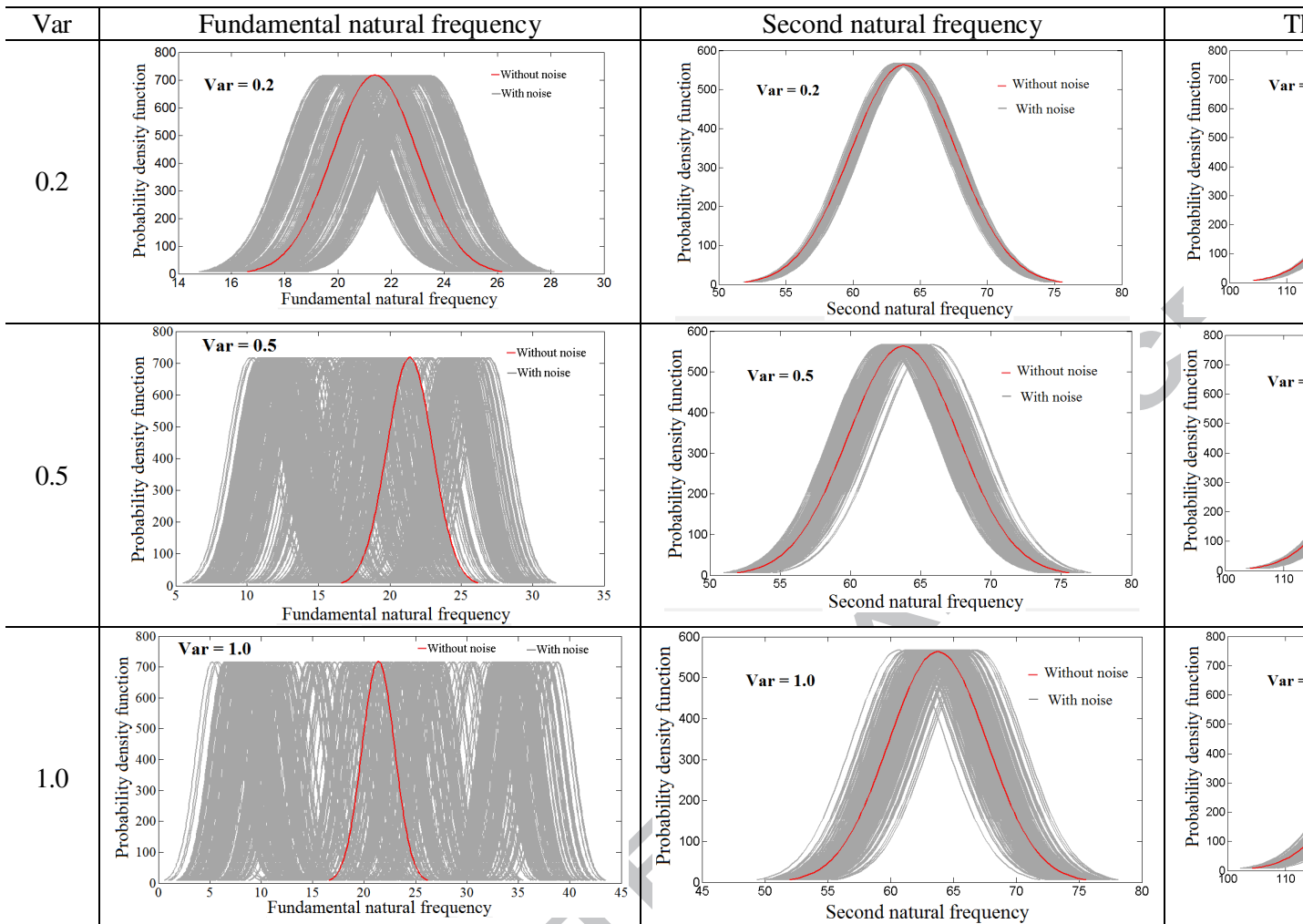


Fig. 12 Effect of noise on PNN based uncertainty quantification for first three natural frequencies (rad/s) of laminated combined variation of ply-orientation angle, thickness, elastic modulus and mass density for angle-ply composite can

is observed as the least sensitive parameter. Interestingly, the stochastic fundamental frequency is identified to be the maximum noise-sensitive compared to higher natural frequencies. The PNN based approach for uncertainty quantification presented in this article can be extended to deal with more complex systems in future.

Acknowledgement

SN and SS gratefully acknowledge the financial support from Lloyd's Register Foundation Centre during this work.

References

- [1] Leissa A.W., *Vibration of plates*, NASA SP-160, 1969.
- [2] Huang C.S., McGee O.G., Leissa A.W., Exact analytical solutions for free vibrations of thick sectorial plates with simply supported radial edges, *Int. J. Solids Struct.*, 31(11), 1609–31, 1994.
- [3] Reddy J.N., A refined nonlinear theory of plates with transverse shear deformation, *Int. J. Solids Struct.*, 20(9-10), 881-896, 1984.
- [4] Liew K.M., Ng T.Y., Wang B.P., Vibration of annular sector plates from three-dimensional analysis, *J. Acoust. Soc. Am.*, 110(1), 233–42, 2001.
- [5] Tornabene F., Viola E., Fantuzzi N., General higher-order equivalent single layer theory for free vibrations of doubly curved laminated composite shells and panels, *Composite Structures*, 104, 94-117, 2013.
- [6] Tornabene F., Fantuzzi N, Bacciocchi M., The local GDQ method applied to general higher-order theories of doubly-curved laminated composite shells and panels: the free vibration analysis, *Composite Structures*, 116, 637–660, 2014.
- [7] Fantuzzi N., Bacciocchi M., Tornabene F., Viola E., Ferreira A.J.M., Radial basis functions based on differential quadrature method for the free vibration analysis of laminated composite arbitrarily shaped plates, *Composites Part B: Engineering*, 78, 65-78, 2015.
- [8] Huang L., Sheikh A.H., Ng C.T., Griffith M.C., An efficient finite element model for buckling of grid stiffened laminated composite plates, *Composite Structures*, 122, 41-50, 2015.

- [9] Shaker A., Abdelrahman W.G., Tawfik M., Sadek E., Stochastic finite element analysis of the free vibration of laminated composite plates, *Computational Mechanics*, 41(4), 493-501, 2008.
- [10] Ganesan R., Free-vibration of composite beam-columns with stochastic material and geometric properties subjected to random axial loads, *Journal of Reinforced Plastics and Composites*, 24(1), 69-91, 2005.
- [11] Lal A., Singh B.N., Stochastic nonlinear free vibration of laminated composite plates resting on elastic foundation in thermal environments, *Computational Mechanics*, 44(1), 15-29, 2009.
- [12] Sefhvand K., Marburg S., Hardtke H.J., Uncertainty quantification in stochastic systems using polynomial chaos expansion, *Int. J. Appl. Mechanics*, 2(2), 305, 2010.
- [13] Naveenthray B., Iyengar N.G.R., Yadav D., Response of composite plates with random material properties using FEM and MCS, *Adv. Compos. Mater.*, 7, 219–237, 1998.
- [14] Salim, S., Yadav, D., Iyengar, N.G.R., Analysis of composite plates with random material characteristics, *Mech. Res. Commun.*, 20(5), 405–414, 1993.
- [15] Onkar A.K., Yadav D., Non-linear response statistics of composite laminates with random material properties under random loading, *Composite Structures*, 60(4), 375–383, 2003.
- [16] Giunta G., Carrera E., Belouettar S., Free vibration analysis of composite plates via refined theories accounting for uncertainties, *Shock and Vibration*, 18, 537–554, 2011.
- [17] Dey S., Mukhopadhyay T., Sahu S.K., Li G., Rabitz H., Adhikari S., Thermal uncertainty quantification in frequency responses of laminated composite plates, *Composites Part B: Engineering*, 80, 186-197, 2015.
- [18] Dey S., Mukhopadhyay T., Adhikari S., Stochastic free vibration analysis of angle-ply composite plates – A RS-HDMR approach, *Composite Structures*, 122, 526-536, 2015.
- [19] Bui T.Q., Nguyen M.N., A moving Kriging interpolation-based meshfree method for free vibration analysis of Kirchhoff plates, *Computers & Structures*, 89(3-4), 380-394, 2011.
- [20] Dey S., Mukhopadhyay T., Adhikari S., Stochastic free vibration analyses of composite shallow doubly curved shells – A Kriging model approach, *Composites Part B: Engineering*, 70, 99-112, 2015.
- [21] Xing Y.F., Wang Y.S., Shi L., Guo H., Chen H., Sound quality recognition using optimal wavelet-packet transform and artificial neural network methods, *Mechanical Systems and Signal Processing*, 66–67, 875-892, 2016.

- [22] Piotrowski A.P., Napiorkowski M.J., Napiorkowski J.J., Osuch M., Comparing various artificial neural network types for water temperature prediction in rivers, *Journal of Hydrology*, 529(1), 302-315, 2015.
- [23] Singh V.P., Chakraverty S., Sharma R.K., Sharma G.K., Modeling vibration frequencies of annular plates by regression based neural network, *Applied Soft Computing*, 9(1), 439-447, 2009.
- [24] Spiridonakos M.D., Chatzi E.N., Metamodeling of dynamic nonlinear structural systems through polynomial chaos NARX models, *Computers & Structures*, 157, 99-113, 2015.
- [25] Dey S., Mukhopadhyay T., Haddad Khodaparast H., Kerfriden P., Adhikari S., Rotational and ply-level uncertainty in response of composite shallow conical shells, *Composite Structures*, 131, 594-605, 2015.
- [26] Dey S., Mukhopadhyay T., Khodaparast H. H., Adhikari S. Fuzzy uncertainty propagation in composites using Gram-Schmidt polynomial chaos expansion, *Applied Mathematical Modelling*, doi:10.1016/j.apm.2015.11.03
- [27] Zjavka L., Wind speed forecast correction models using polynomial neural networks, *Renewable Energy*, 83, 998-1006, 2015.
- [28] Gómez-Ramírez E., Najim K., Ikonen E., Forecasting time series with a new architecture for polynomial artificial neural network, *Applied Soft Computing*, 7(4), 1209-1216, 2007.
- [29] Zhang Y., Yin Y., Guo D., Yu X., Xiao L., Cross-validation based weights and structure determination of Chebyshev-polynomial neural networks for pattern classification, *Pattern Recognition*, 47(10), 3414-3428, 2014.
- [30] Xin Yu, Qingfeng Chen, Convergence of gradient method with penalty for ridge polynomial neural network, *Neurocomputing*, 97, 405-409, 2012.
- [31] Xin Yu, Lixia Tang, Qingfeng Chen, Chenhua Xu, Monotonicity and convergence of asynchronous update gradient method for ridge polynomial neural network, *Neurocomputing*, 129, 437-444, 2014.
- [32] Seok-Beom Roh, Tae-Chon Ahn, Witold Pedrycz, Fuzzy linear regression based on polynomial neural networks, *Expert Systems with Applications*, 39(10), 8909-8928, 2010.
- [33] Roh S.B., Oh S.K., Pedrycz W., Design of fuzzy radial basis function-based polynomial neural networks, *Fuzzy Sets and Systems*, 185(1), 15-37, 2011.
- [34] Huang W., Oh S.K., Pedrycz W., Design of hybrid radial basis function neural networks (HRBFNNs) realized with the aid of hybridization of fuzzy clustering method (FCM) and polynomial neural networks (PNNs), *Neural Networks*, 60, 166-181, 2014.

- [35] Oh S.K., Kim W.D., Park B.J., Pedrycz W., A design of granular-oriented self-organizing hybrid fuzzy polynomial neural networks, *Neurocomputing*, 119, 292-307, 2013.
- [36] Fazel Zarandi M.H., Türksen I.B., Sobhani J., Ramezani-pour A.A., Fuzzy polynomial neural networks for approximation of the compressive strength of concrete, *Applied Soft Computing*, 8(1), 488-498, 2008.
- [37] Maric I., Optimization of self-organizing polynomial neural networks, *Expert Systems with Applications*, 40(11), 4528-4538, 2013.
- [38] Dorn M., Braga A.L.S., Llanos C.H., Coelho L.S., A GMDH polynomial neural network-based method to predict approximate three-dimensional structures of polypeptides, *Expert Systems with Applications*, 39(15), 12268-12279, 2012.
- [39] Meirovitch L., *Dynamics and Control of Structures*, John Wiley & Sons, NY, 1992.
- [40] Dey S., Karmakar A., Natural frequencies of delaminated composite rotating conical shells - A finite element approach, *Finite Elements in Analysis and Design*, 56, 41-51, 2012.
- [41] Dey S., Karmakar A., Free vibration analyses of multiple delaminated angle-ply composite conical shells – A finite element approach, *Composite Structures*, 94(7), 2188-2196, 2012.
- [42] Bathe K.J., *Finite Element Procedures in Engineering Analysis*, PHI, New Delhi, 1990.
- [43] Schetin V., Polynomial neural networks learnt to classify EEG signals, NIMIA-SC2001 - 2001 NATO Advanced Study Institute on Neural Networks for Instrumentation, Measurement, and Related Industrial Applications: Study Cases Crema, Italy, 9-20 October 2001.
- [44] Mellit A., Drif M., Malek A., EPNN-based prediction of meteorological data for renewable energy systems, *Revue des Energies Renouvelables*, 13(1), 25 – 47, 2010.
- [45] Oh S.K., Pedrycz W., Park B.J., Polynomial neural networks architecture: Analysis and design, *Comput. Electr. Eng.*, 29(6), 703-725, 2003.
- [46] Lyon A, Why are Normal Distributions Normal? *The British Journal for the Philosophy of Science*, 65 (3) 621-649, 2014.
- [47] Mukhopadhyay T., Chowdhury R., Chakrabarti A. Structural damage identification: a RS-HDMR approach, *Advances in Structural Engineering*, 2016, doi: 10.1177/1369433216630370.

- [48] Dey S., Mukhopadhyay T., Spickenheuer A., Adhikari S., Heinrich G., Bottom up surrogate based approach for stochastic frequency response analysis of laminated composite plates, *Composite Structures*, 140, 712–727, 2016.
- [49] Mukhopadhyay T., Dey T.K., Chowdhury R., Chakrabarti A., Structural damage identification using response surface based multi-objective optimization: A comparative study, *Arabian Journal for Science and Engineering*, 40(4), 1027-1044, 2015.
- [50] Mukhopadhyay T., Naskar S., Dey S., Adhikari S., On quantifying the effect of noise in surrogate based stochastic free vibration analysis of laminated composite shallow shells, *Composite Structures*, 140, 798–805, 2016.
- [51] Qatu M.S., Leissa A.W., Natural frequencies for cantilevered doubly curved laminated composite shallow shells, *Composite Structures*, 17, 227–255, 1991.
- [52] Qatu M.S., Leissa A.W., Vibration studies for laminated composite twisted cantilever plates, *International Journal of Mechanical Sciences*, 33(11), 927–940, 1991.